

# Human EEG Correlates of Spatial Navigation within Egocentric and Allocentric Reference Frames

Markus Plank<sup>1</sup>, Hermann J. Müller<sup>2</sup>, Julie Onton<sup>3</sup>, Scott Makeig<sup>3</sup>,  
and Klaus Gramann<sup>3</sup>

<sup>1</sup> Institute for Neural Computation, University of California San Diego,  
9500 Gilman Drive #0523, La Jolla, CA 92093, USA

<sup>2</sup> Allgemeine und Experimentelle Psychologie,  
Ludwig-Maximilians-Universität München, Leopoldstr. 13, 80802 München, Germany  
<sup>3</sup> Swartz Center for Computational Neuroscience, University of California San Diego,  
9500 Gilman Drive #0559, La Jolla, CA 92093, USA  
mplank@ucsd.edu

**Abstract.** We investigated the impact of path complexity on brain dynamics of subjects who preferentially use an egocentric (Turners) or an allocentric (Nonturners) reference frame during spatial navigation. Participants indicated a return bearing direction ('point-to-origin') following visual presentation of virtual tunnel passages, varying with respect to the complexity of the outbound path. High-density electroencephalographic activity was recorded continuously and spatially filtered with Independent Component Analysis. For Turners, rotations and translations were associated with decreased and increased (8-12 Hz) alpha activity in occipito-parietal cortex, whereas Nonturners displayed increased alpha within cortical areas along the ventral pathway, as well as in retrosplenial cortex, an area supporting bidirectional exchange of information between parietal and medial temporal regions. Both groups displayed complexity-related modulations of frontal midline (4-8 Hz) theta activity. Findings extend results of hemodynamic imaging and neuropsychological studies on spatial navigation and emphasize the need for considering individual proclivities when investigating human navigation performance.

**Keywords:** path integration, reference frames, egocentric, allocentric, EEG, ICA, Independent Component Analysis, source reconstruction, ERSP.

## 1 Introduction

Spatial navigation constitutes a sub-category of spatial cognition and denotes the capacity to plan and execute goal-directed paths based on the computation, maintenance, and utilization of internal representations of the environment [1]. These representations comprise the location of threats, rewards, and other agents and their spatial relations, as well as one's own position with respect to the represented entities [2]. The navigator's position and orientation can be inferred by *path integration*, i.e., the continuous integration of local translations and rotations from movement cues [3].

The integration of spatial information during path integration takes place within dissociable, but interacting spatial reference frames. Most generally, a distinction is made between a self-centered *egocentric* reference frame and an environment-centered *allocentric* reference frame [2, 4]. Within the former, *egocentric* self-to-object *distances* and *bearings* are coded independently of the global layout of the environment, with respect to the three intrinsically defined axes of the navigator (front–back, right–left, and up–down). As the navigator moves, egocentric parameters have to be updated with each consecutive step by adding the displacement vector of an object (relative to the navigator) to their previous egocentric position vectors. In other words, the world constantly changes, whereas the navigator remains spatially fixed in the center of the reference system [5]. The resulting spatial representation therefore can be characterized as being highly dynamic and transient. Behavioral studies in triangle-completion have indeed shown that with increasing path complexity in terms of overall length and/or number of turns, spatial updating of egocentric parameters becomes more and more challenging, resulting in larger errors and increased response times [6, 7].

By contrast, an *allocentric reference frame* establishes a coordinate system with an origin and a reference direction external to the navigator. Within the resulting *allocentric locational representation* inter-object relations are represented independent of the navigator's current position and/or orientation, exclusively related to the external reference properties, with coordinate axes being defined by the global layout of the environment. Also, the navigator himself is represented in terms of position, but without any orientation. The use of an allocentric reference frame requires the moving navigator to constantly update his position but not his orientation since all *allocentric distances* and *allocentric bearings* remain stationary as the navigator proceeds. Recent experiments have provided initial evidence for spatial accuracy being considerably high even after long and winding outbound trajectories whenever participants represent the traversed pathway within an allocentric reference frame [8].

The subject's choice of navigating within an egocentric or an allocentric reference frame partly depends on the sensory modality activated during navigation [9], as well as the perspective from which an environment is initially encountered and learned [10, 11]. Further, several studies have provided rich evidence for the existence of intraindividually stable proclivities in using either an egocentric or an allocentric frame during visual path integration [12-14]. By developing a task that allowed for a categorization of subjects with respect to their preference for using an egocentric or an allocentric reference frame [12], it was possible to differentiate *Turners*, who preferentially use an egocentric reference frame, and *Nonturners*, who preferentially use an allocentric reference frame for spatial navigation (see Figure 1). This segregation was neither attributable to differences in the feeling ofvection nor to group-specific eye movement patterns during navigation through sparse visual environments [15].

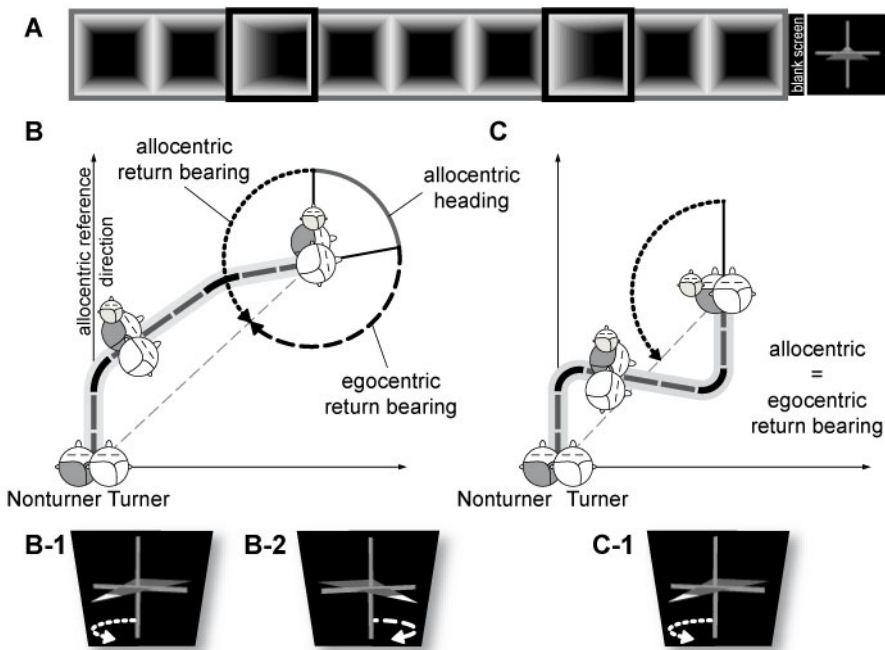


**Fig. 1.** [A] Snapshot of a tunnel with straight and curved segments (framed black), providing visual information on forward motion from a first person perspective; [B] When traversing tunnels with two turns bending to the same side, return bearings of Turners (using an egocentric reference frame, white heads) and Nonturners (using an allocentric reference frame, dark grey heads) are initially aligned, but diverge with changes in perceptual heading along the trajectory. At the end, Nonturners rotate the virtual arrow so that it points 120° to their left (**B-1**), whereas Turners adjust the arrow 120° to their right (**B-2**). The homing responses indicate that Nonturners adjust the homing arrow with respect to the allocentric reference direction (small light grey head) corresponding to the allocentric return bearing, whereas Turners respond with respect to their final cognitive heading corresponding to the egocentric return bearing; [C] For tunnels with two opposite turns of equal angularity, both systems are re-aligned after the second turn, resulting in identical arrow adjustments for Turners and Nonturners (**C-1**), based on the equivalence of egocentric and allocentric return bearings.

### 1.1 Cortical Structures and Processes Subserving the Use of Egocentric and Allocentric Reference Frames

The conceptual dissociation of egocentric and allocentric reference frames is further reflected by structural as well as functional differences in the underlying neural substrate [11, 16]. Under natural circumstances, both systems interact during the encoding and retrieval of spatial knowledge. Based on incoming visual flow, information regarding one's ego-motion is extracted and further processed along the *dorsal pathway* within medial occipital and posterior parietal areas [17], with the latter co-ordinating transformations between various reference frames (e.g., eye-, body-, head- or world-centered) [18, 19]. Firing patterns of parietal cells are affected by combinations

of velocity, head direction, and visual stimuli, bearing resemblance to findings on parietal lesions in humans associated with improper integration of heading information [20, 21].

Additional cells that respond selectively to position-independent heading are located in cingulate cortex [22]. Particularly its posterior portion (retrosplenial cortex) is interconnected with posterior parietal cortex, superior temporal sulcus, as well as subcortical structures [23, 24]. The retrosplenial cortex plays a central role for the proper integration of head direction and information on heading-invariant landmark information arising from place cells in medial temporal, particularly hippocampal structures. Place cells in the hippocampal formation have been found to respond to an animal's location in space independent of its current orientation [25], giving rise to the assumption that certain aspects of the allocentric reference frame reside in these areas [26]. Beyond object-based processing along the *ventral pathway*, hippocampal structures also receive context-independent position information upstream from entorhinal grid cells. In contrast to place cells, these cells establish a map of the environment that is only initially anchored to external landmarks, but persists in their absence, which might contribute central elements for the long-term storage of spatial structures [27]. Finally, parietal as well as hippocampal structures possess interconnections to prefrontal regions that are associated with reference-frame unspecific functions of spatial working memory comprising maintenance of encoded information as well as goal-directed planning [28].

The temporal dynamics of activity within these areas during the acquisition, consolidation, and retrieval of spatial knowledge may be investigated by means of high-density electroencephalography (EEG). Generally, spontaneous EEG activity is constituted by uncoupled intracortical sources producing random oscillatory activity in a wide frequency range. Sensory stimulation causes a coupling of these generators, resulting in temporally synchronous and coherent oscillations. In the context of spatial navigation, alpha and theta frequency bands constitute the most extensively studied oscillations, since they have repeatedly been shown to correlate with mental states and strategies as well as stimulus characteristics. Activity in the (4 – 8 Hz) theta frequency band is directly related to memory maintenance and increases with task difficulty [29]. Particularly during heading changes pronounced theta activity has been detected [30] which might serve as gating mechanism during information encoding, consolidation and retrieval [31]. By contrast, activity in the (8 – 13 Hz) alpha frequency band has several functional correlates reflecting sensory, motor, and memory functions [32]. Alpha arises primarily from posterior sites, including occipital, parietal, and posterior temporal regions. Decreased alpha constitutes a valid signature of activation or cognitive preparedness of the cortical domain for processing of task-related information [33].

However, the EEG signal measured on the scalp surface does not originate on-site, i.e., directly beneath a certain electrode, but can be characterized as a sum of many electrical processes, including those with neural or muscular origin [34, 35]. The far-field potential arising from each of these synchronized cellular assemblies spreads via volume conduction and is recorded, to a greater or lesser extent, by every surface electrode instantaneously. Independent Component Analysis (ICA) has been successfully applied to EEG data to separate these mixed signals into spatially fixed but temporally independent processes [36].

## 1.2 Aims of the Current Study

Bringing together the excellent temporal resolution of high-density EEG recordings, seminal progress in data mining techniques, as well as VR technology, the current study aimed at the identification of generator sources of brain activity as well as macroscopic oscillatory dynamics during path integration within egocentric and allocentric reference frames. The difference in primitive parameters between egocentric and allocentric spatial representations suggests that they are processed within distinct neural circuits (dorsal vs. ventral pathway). On the other hand, following the remarks of Burgess [4] as well as initial results of Gramann et al. [13], egocentric and allocentric systems might be activated in parallel. This parallel processing might be reflected by specific dynamics within distinct brain areas responsible for the processing of reference frame-specific spatial information, as well as reference frame-unspecific activation associated with the coordinated transformation of spatial information between reference frames. Based on this question, the systematic variation of the path layout allowed, for the first time, the analysis of how brain dynamics within areas associated with reference frame-specific as well as -unspecific cognitive processing are modulated by changes in outbound path complexity.

## 2 Material and Methods

Thirty-seven male students recruited from the Ludwig-Maximilians-University Munich, Germany, participated in the Experiment (age ( $M \pm SD$ ) =  $24.64 \pm 3.52$  years). Participants were either paid 8€ per hour or received course credit for taking part in the experiment. All subjects had normal or corrected to normal vision and reported no history of neurological disorder.

Prior to the main experiment, subjects were classified for their preferred spatial strategy (Nonturner vs. Turner). In this categorization task, participants sat in an electromagnetically shielded room, 170 cm in front of a flat projection screen (120 x 90 cm), which was illuminated by a Sanyo PLC-XU47 projector (800 x 600 pixels, 275W, 60 Hz). The screen center was horizontally aligned with the participant's line of sight. Visual stimulation covered a visual field of view of approx.  $41^\circ \times 41^\circ$ . Participants passively traversed 30 tunnels with one single turn of varying angle. Tunnels were composed of an initial straight segment followed by a curved segment and two final straight segments. Movement was simulated solely by optic flow, with a constant speed of 2.27 seconds/segment. At the end of a passage two virtual arrows were displayed simultaneously that represented the correct homing response based on an allocentric or an egocentric reference frame. In a forced-choice task, participants had to spontaneously decide which of the two arrows pointed back to the starting point of their passage (see Figure 1B for examples of homing arrows).

Within three blocks of 10 trials each turning angles gradually decreased, so that egocentric and allocentric arrows converged, resulting in increasing task difficulty. In order to take part in the main experiment, participants had to consistently (i.e., more than 83% of the trials) select the allocentric or egocentric arrow to be categorized as Nonturners or Turners, respectively. All subjects selected for the main experiment demonstrated consistent choice of one or the other reference frame (Turners  $M \pm SD$  =

99%  $\pm$  0.02%), Nonturners M $\pm$ SD = 96%  $\pm$  0.04%; correlation between preferred strategy and strategy-specific arrow choice:  $r(37) = .997$ ,  $p < .00001$ ). 20 subjects were categorized as *Turners* (egocentric) and 17 as *Nonturners* (allocentric). All Turners were right-handed, four Nonturners were left-handed.

The main experimental session included 20 blocks of 9 tunnels each with minor in-between breaks. During the experiment tunnels with one turn and two turns were presented. The task of the subjects was to maintain orientation while being passively transported along the tunnel passage and to subsequently rotate a simulated 3-D arrow to point directly back to the starting point of the trajectory ('point-to-origin'). In order to minimize EEG movement artifacts, arrow adjustment was accomplished by pressing and holding right and left mouse buttons. Pressing the center mouse button confirmed the adjustment.

Tunnels with one turn consisted of five segments (segment duration = 1875 ms), with the two initial and two final straight segments enclosing the turning segment of varying angle. Tunnels with two turns had a total of nine segments (turn segments located in segments 3 and 7). Since depth of sight was limited to the upcoming 1.5 segments, the placement of the first turn in segment 3 ensured that participants could not determine the direction and amount of the first rotation directly at the beginning of the presentation. Further, we inserted three straight segments between the first and the second turn, so that subjects were not able to predict whether they were traversing a tunnel with five or with nine segments until either the end of the passage appeared or the tunnel continued through a second turn. In 10% of the trials participants received strategy-specific feedback on homing accuracy (based on the a priori categorized preference).

The main experiment was composed of 180 trials, constituting a factorial combination of 2 lengths/number of turns (5 segments, one turn; 9 segments, two turns)  $\times$  2 sides of end position (left; right)  $\times$  4 categorical eccentricities of end position<sup>1</sup> (15°, 30°, 45°, and 60°, each with variation of  $\pm 2^\circ$  in order to prevent stereotypical homing responses)  $\times$  10 repetitions per condition, plus 20 filler trials (start of each block) being straight tunnels.

The EEG was continuously recorded with a high-density array of 128 Ag/AgCl electrodes corresponding to the international 5%-system [37]. Impedance was kept below 7 k $\Omega$ . The signal was filtered online with a band-pass of .016–100 Hz, and digitized at a sampling rate of 500 Hz. An additional electrode was placed on the infraorbital ridge of the left eye to record the vertical electro-oculogram (EOG). Data were analyzed off-line with the freely available MATLAB-toolbox EEGLAB [38]. After downsampling to 250 Hz data were digitally filtered to remove frequencies above 50 Hz and re-referenced to linked mastoids. Continuous data were first screened for atypical (excessive peak-to-peak deflections or bursts of electromyographic activity) epochs. The remaining data were decomposed by extended infomax ICA using binica [39] as implemented in EEGLAB.

<sup>1</sup> Eccentricity of end position was computed within an allocentric reference frame (with respect to the initial straight segment of the tunnel passage). Different end positions corresponded to different turning angles, e.g., the end position of 15° eccentricity required either a single turn of 30°, or two turns to the same side of 15° and 10°, or two opposite turns of 30° and -30°.

For every participant, ICA returned 128 maximally independent components. Subsequently, DIPFIT2 routines from EEGLAB were applied to fit single equivalent dipole models to the IC scalp topographies using a four-shell spherical head model [40]. Components with bilaterally distributed scalp maps were fit with a dual dipole model using a symmetrical constraint. Components with an equivalent dipole model explaining less than 85% variance of the measured scalp maps and components that reflected muscle activity, electrocardiogram, or eye movements were excluded from further analysis.

After decomposition, the data were segmented into overlapping epochs of 2875 ms (length of one tunnel segment plus 500 ms pre- and 500 ms post-stimulus time window) and normalized for between subject comparison by subtracting mean log power from single-trial log power. Subsequently, data were baseline-corrected by subtracting the average EEG spectrum of all trials, beginning with the second tunnel segment and ending with the penultimate segment of the tunnel passage (for tunnels with one turn: Segment 4; for tunnels with two turns: Segment 8). Mean Event-Related Spectral Perturbations (ERSP) were computed by subtracting the 2-D (frequency-by-latency) mean log power spectrum of the baseline from the mean log power at each time point of the experimental trials [41, 42]. This approach provides insights into event-related brain dynamics in a wide frequency range for the whole time course of the tunnel passage.

IC processes were clustered across subjects by means of a joint distance measure, based on power spectra, event-related potentials, scalp projections, equivalent dipole locations, mean ERSP, and inter-trial coherence for each selected IC from each subject. The resulting component distances were clustered using a *K-means* cluster algorithm as implemented in the EEGLAB toolbox (see [34] for further details).

### 3 Results and Discussion

Strategy-specific expected and observed angular adjustments were highly correlated for both Nonturners and Turners. For Turners, using an egocentric reference frame, correlation coefficients were comparable at all complexity levels ( $r_{1\text{-turn}}(80) = .950$ ;  $r_{2\text{-turns(same)}}(70) = .924$ ;  $r_{2\text{-turns(opposite)}}(60) = .899$ ; all  $p < .0001$ ). This pattern was identical for Nonturners, using an allocentric reference frame ( $r_{1\text{-turn}}(120) = .972$ ;  $r_{2\text{-turns(same)}}(72) = .937$ ;  $r_{2\text{-turns(opposite)}}(48) = .895$ ; all  $p < .0001$ ). Although tunnels varied on a trial-to-trial basis with respect to the turning angle and overall length, the pronounced correlation between expected and observed homing responses confirms the subjects' capability to extract directional information from purely visual flow on local translations and rotations. Given that the underlying egocentric and allocentric representations of Turners and Nonturners were of comparable spatial accuracy, it was of interest, if the strategy groups differed in terms of the underlying cortical structures and spectral dynamics within these areas during navigation.

A total of 599 independent component (IC) processes were retained (see Figure 2); 275 from Nonturner subjects, and 324 from Turner subjects. The number of ICs ranged from 9 to 28, with both groups displaying a mean number of retained components of 16.2 (difference between strategy groups:  $\chi^2_{df=1} = 1.05$ ,  $p > .05$ ). 22 IC clusters were obtained. Two clusters mirrored horizontal and vertical EOG activity, and

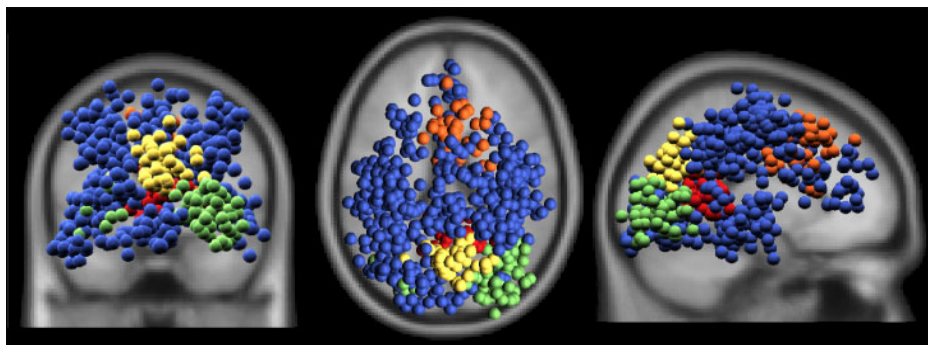


**Fig. 2.** Reconstructed equivalent model dipole locations of the 599 functional IC processes (dipoles related to eye movements are not shown); Blue spheres display equivalent model dipole locations of IC processes in 16 clusters without significant ERSP differences between strategy groups and/or complexity levels; (green) cluster located in or near bilateral occipital gyrus; (yellow) cluster in or near right precuneus; (red) cluster in or near posterior cingulate/retrosplenial cortex; (orange) cluster in or near right cingulate gyrus

20 clusters reflected brain processes (see Figure 2). Stereotaxic Talairach coordinates, residual variances, Brodmann Areas, the number of Nonturner and Turner subjects, as well as the number of ICs within four representative clusters are summarized in Table 1. The results replicated and extended previous findings regarding the spectral dynamics of distinct brain areas during spatial navigation [13, 43] by further analyzing the brain dynamics dependent on the complexity of the outbound path. At all complexity levels,

**Table 1.** Properties of 4 representative IC clusters, sorted from posterior to anterior IC cluster sites (along the y-axis). Columns provide information regarding (1) the location of the cluster centroids in Talairach space (x-y-z). All reconstructed clusters for each condition were anatomically specified within the stereotaxic coordinate system of Talairach and Tournoux using the Talairach demon software [45], returning the coordinates of the nearest grey-matter point. Further, the table provides information regarding (2) the residual variance (RV, in %) of the reconstructed cluster centroids, and (3) their anatomical region defined in the Brodmann Area system [46]. Finally, the table gives information regarding the number of Nonturner and Turner subjects ( $S_{NT}$ ,  $S_T$ ), as well as the amount of Nonturner and Turner Independent Components ( $IC_{NT}$ ,  $IC_T$ ) within each cluster.

Cl	Talairach			RV [%]	Brodmann Areas	$S_{NT}$	$S_T$	$IC_{NT}$	$IC_T$
	x	y	z						
1	29	-79	-1	3.41	BA 18 R (bilat.) inferior occipital gyrus	13	17	22	33
2	4	-69	30	2.65	BA 7/31 R (midline) precuneus	13	15	16	23
3	5	-49	11	5.37	BA 29/30 R posterior cingulate/ retrosplenium	9	9	16	17
4	7	13	38	3.56	BA 32 R cingulate gyrus	12	10	20	14

Turners and Nonturners displayed comparable deflections from baseline in or near primary/secondary visual cortex (Independent Component Cluster ICC 1, BA 17/18) reflecting activity accompanying visual processing from a first-person perspective. Whereas translational information was associated with relative synchronization of the alpha frequency band (near 10 Hz), the combined translational/rotational information during tunnel turns resulted in alpha desynchronization (see Figure 3-A). The desynchronization of alpha has been associated with increased cognitive processing during relevant time-points of a given task [31, 44].

Despite identical visual processing of Turners and Nonturners, spectral dynamics displayed distinct patterns as information was processed along the dorsal stream, particularly in or near posterior parietal cortex (ICC 2, BA 7/31). Whenever the second turn bended into the same direction, Turners exhibited a relative alpha desynchronization in or near posterior parietal cortex upon viewing the second turn prevailing until they entered the turning segment. By contrast, Nonturners' alpha activity did not differ from baseline during this time period (see Figure 4-A). In posterior parietal cortex the fusion of multiple egocentric reference frames is accomplished, further projecting to motor structures in order to coordinate appropriate movements [47]. In concert with retrosplenial cortex, posterior parietal cortex further integrates heading changes [48], conveying allocentric aspects of space [49]. Since the homing response of Turners closely resembles the egocentric return bearing that requires the updating of cognitive heading during rotations, the more pronounced alpha desynchronization of Turners points to increased cognitive effort during the integration of future heading during turns [50, 51]. The homing response of Nonturners, by contrast, matches the allocentric return bearing that, by definition, does not require the integration of heading. The absence of alpha desynchronizations during turns, however, does per se not exclude the integration of egocentric information for Nonturners. Rather, the processing of this information is not as accentuated during turns to the same side as for Turners.

For tunnel configurations with two *opposite* turns of equal angularity (Figure 4-B), Turners and Nonturners displayed significant alpha desynchronization in posterior parietal regions upon viewing the second turn. But whereas for Nonturners alpha power increased to baseline as they actually entered the turn, for Turners alpha desynchronization persisted until the end of the second turn.

Given that the general side of egocentric self-to-object relations (including the egocentric return bearing) can be maintained when traversing subsequent turns to the same side but that opposite turns necessitate the whole environmental array to be shifted with respect to the intrinsic axis of the navigator, the prolonged processing of rotational information for Turners might be associated with a cognitively highly demanding spatial updating of egocentric return bearing as well as heading during the second, opposite turn [3]. Our results indicate that this shift of relative self-to-object relations is accomplished in posterior parietal cortex, in line with previous studies [e.g., 51].

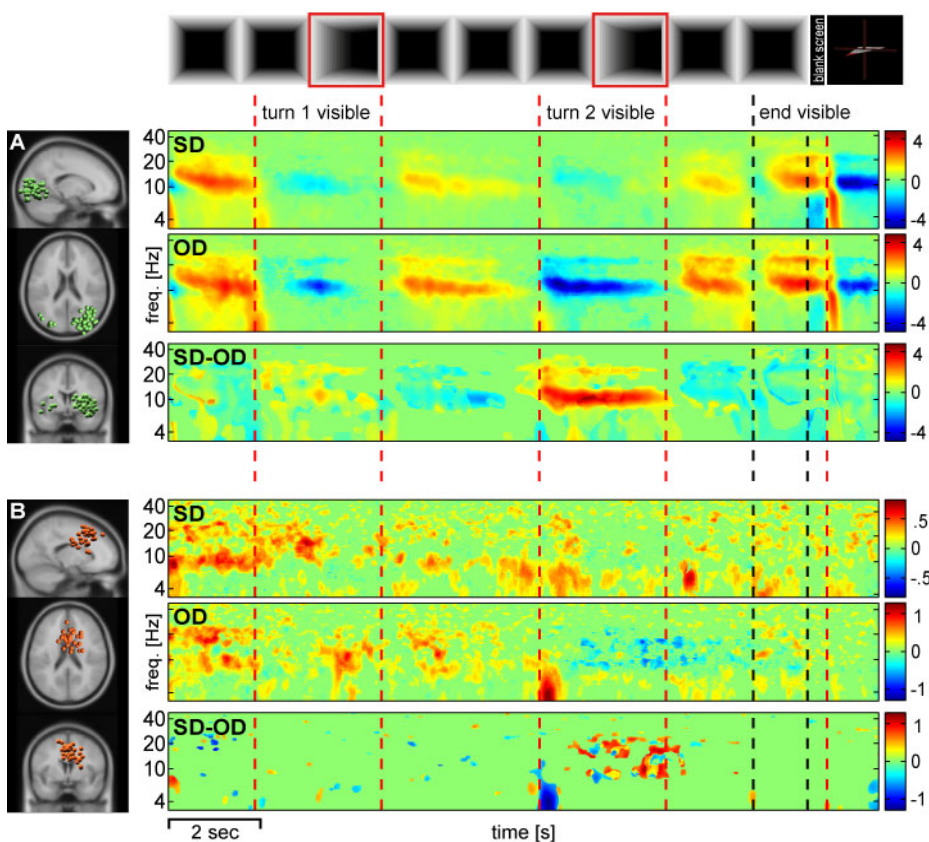


**Fig. 3.** [A] Mean ERSP images for a cluster of independent source processes located in or near bilateral lingual gyrus (BA 17/18) revealing task-dependent changes in spectral power during spatial navigation through tunnel passages containing two turns into the same direction (**SD**) and into opposite directions (**OD**). Cluster centroid mean ERSPs are plotted in log-spaced frequencies from 3 – 45 Hz. Green indicates no significant ( $p > .001$ ) difference in mean log power (dB) from baseline. Warmer colors indicate significant increases (synchronizations,  $\text{dB} > 0$ ), and colder colors decreases (desynchronization,  $\text{dB} < 0$ ) in log power from baseline. ERSP differences between tunnel configurations are shown in panel (**SD-OD**) ( $p < .0001$ , corrected for multiple comparisons); Important time points of the tunnel passage are marked with dashed lines, indicating the period when participants approached and traversed turns, or encountered the end of the tunnel, as well as the initial 1.38 seconds of the virtual homing vector adjustment; [B] ERSP images for a cluster of IC processes located in or near right cingulate gyrus (BA 32), separately for tunnels with two turns into the same direction (**SD**), and two turns into opposite directions (**OD**). Panel (**SD-OD**) depicts ERSP differences between tunnel configurations.

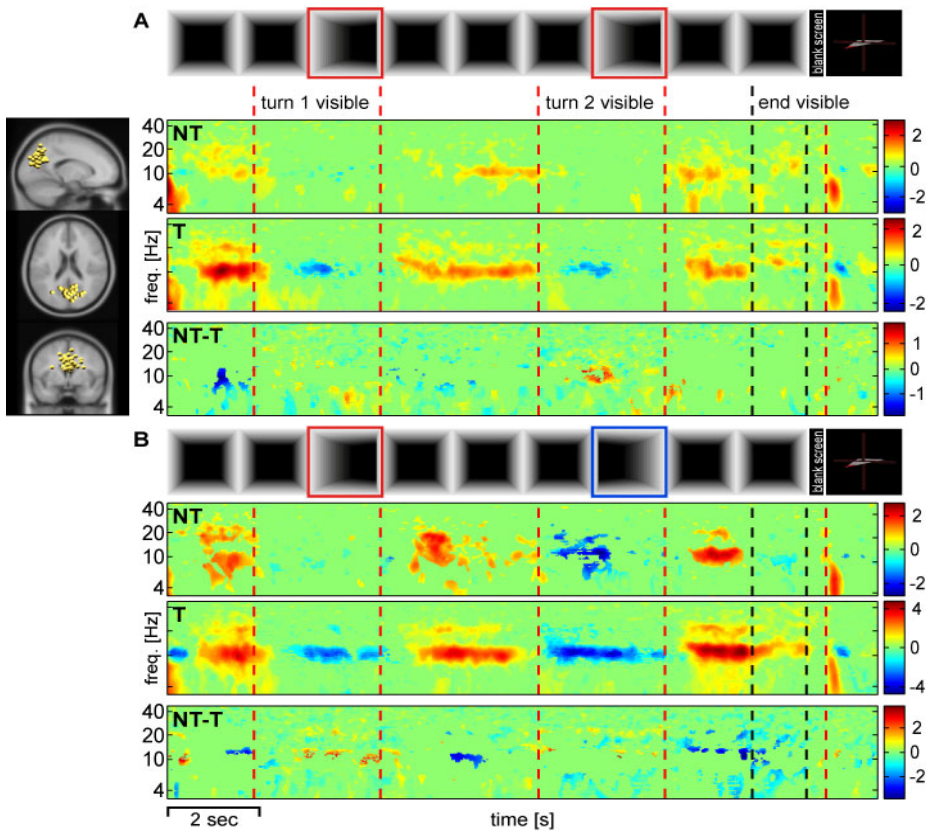


**Fig. 4.** Mean event-related spectral perturbation (ERSP) images for an IC cluster located in or near midline precuneus (BA 7/31) revealing task-dependent changes in spectral power during spatial navigation through tunnel passages containing two turns into the same direction [A] and into different directions [B], with separate plots for Nonturners, navigating within an allocentric reference frame (NT), and Turners, using an egocentric reference frame (T). ERSP differences between strategy groups are shown in panels (NT-T) ( $p < .0001$ , corrected for multiple comparisons). For further explanation see Figure 2.

As can be seen from Figure 5, prior to entering as well as during the second, opposite turn, only Nonturners demonstrated significantly increased alpha desynchronization in or near retrosplenial cortex (ICC 3, BA 29/30). Since actual perceptual heading (egocentric) and cognitive heading (allocentric) diverge during this time period, this finding might be associated with a more pronounced inhibition of processing egocentric visuospatial information in order to prevent interference with maintaining two spatial reference frames in parallel [52]. However, it remains an open question why this pattern is only prevalent during the second, opposite turn. In addition to the strategy-specific spectral dynamics of the (near 10 Hz) alpha frequency band in occipital and parietal cortices, subjects displayed comparable theta (near 4 – 8 Hz) synchronizations in or near medial frontal cortex that occurred at specific time-points of the trajectory, e.g., as turns or the end of the passage became visible (see Figure 3-B).

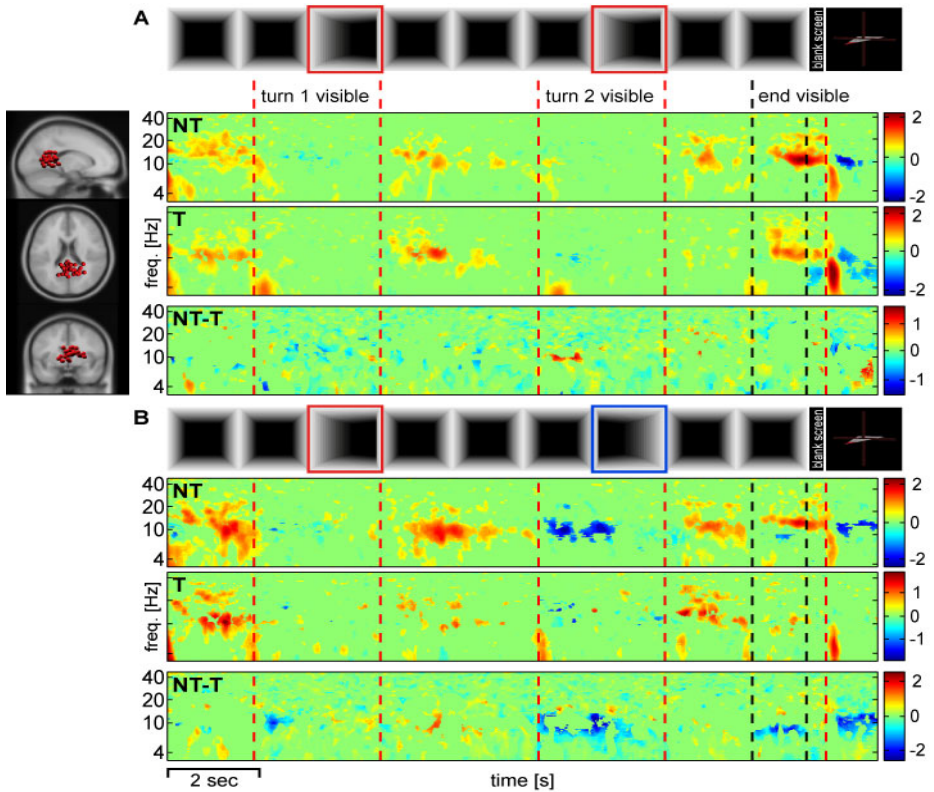


**Fig. 5.** Mean event-related spectral perturbation (ERSP) images for an IC cluster located in or near midline posterior cingulate cortex (retrosplenium, BA 29/30) revealing task-dependent changes in spectral power during spatial navigation through tunnel passages containing two turns into the same direction [A] and into different directions [B], with separate plots for Non-turners, navigating within an allocentric reference frame (NT), and Turners, using an egocentric reference frame (T). ERSP differences between strategy groups are shown in panels (NT-T) ( $p < .0001$ , corrected for multiple comparisons). For further explanation see Figure 2.

Importantly, for tunnels with two turns the actual time-point of the final theta synchronization in or near anterior cingulate cortex (ICC 4, BA 32) was determined by the layout of the outbound path: In case of two turns bending into the same direction, the final theta synchronization appeared not until after the final turn, resembling the pattern for tunnels with one turn (not shown). For tunnels with two *opposite* turns of equal angularity, it already emerged upon viewing the second turn. Since turns of opposite tunnel configurations always were of equal angularity, participants might have determined the angle of the upcoming second turn even before entering the turn itself. This could have prevented the occurrence of a final theta burst anteceding the final turning segment. By contrast, whenever the second turn bent into the *same direction*, angles were not equal but several path layouts could end on a certain eccentricity. Here, participants first had to process the rotational information during the second turn before reliably updating their heading and return bearing [30]. Therefore, this

activity pattern in frontal theta might index cognitive effort during spatial updating based on the retrieval of the previously traversed tunnel segments [53, 54].

## 4 Conclusion and Perspective

To the author's knowledge, this is the first study investigating EEG brain dynamics accompanying the use of an allocentric or egocentric reference frame during path integration on multiple complexity levels. The individual preference for the use of an egocentric or an allocentric reference frame was accompanied by dissociable brain dynamics in distinct cortical networks. Turners and Nonturners displayed differential spectral activation patterns of the alpha frequency band (near 8 – 12 Hz) within several IC clusters in or near occipital, occipito-parietal as well as posterior parietal cortices. Additional differences were found in or near retrosplenial cortex. These differences might be linked to a strategy-specific updating of representational primitives such as egocentric and allocentric return bearings and distances as well as allocentric heading from integration of rotational and/or translational information. Besides strategy-specific modulations, Turners and Nonturners displayed comparable, complexity-modulated activation patterns of the theta frequency band (near 4 – 8 Hz) in or near medial frontal cortex most likely mirroring increased cognitive effort during memory retrieval of previously traversed segments.

Taken together, the results suggest that the complexity of the traversed pathway in terms of the direction of subsequent turns has differential effects on macroscopic brain dynamics of subjects preferring to navigate within an egocentric or an allocentric reference frame. Since identical visual stimulation was found to provoke differential activity in brain areas linked to reference-specific cognitive processes, individual proclivities should be considered more carefully in studies on spatial navigation. Future research has to address how the present results transfer to more general navigation tasks, e.g., when additional vestibular and proprioceptive information or landmarks are available. Fully immersive 3-D VR systems utilizing mobile brain imaging [55] might constitute the seminal basis for further investigation of complexity effects on behavioral and electrocortical correlates of allocentric and egocentric navigation under more natural conditions.

**Acknowledgements.** This research was supported by the German Research Foundation (DFG GR2627/2-1), the German Academic Exchange Service (DAAD), the Boehringer-Ingelheim-Fonds, and by the G.-A.-Lienert-Foundation for Promotion of Young Researchers in Biopsychological Methods. The authors further want to thank the anonymous reviewers for their help in improving this article, as well as the participants for their time and interest in this work.

## References

1. Gallistel, C.R.: *The organization of learning*. MIT Press, Cambridge (1993)
2. Klatzky, R.L.: Allocentric and egocentric spatial representations: Definitions, distinctions, and interconnections. In: Freksa, C., Habel, C., Wender, K.F. (eds.) *Spatial Cognition 1998. LNCS (LNAI)*, vol. 1404, pp. 1–17. Springer, Heidelberg (1998)

3. Loomis, J.M., Klatzky, R.L., Golledge, R.G., Philbeck, J.W.: Human navigation by path integration. In: Golledge, R.G. (ed.) *Wayfinding behavior. Cognitive Mapping and Other Spatial Processes*, pp. 125–151. John Hopkins Univ. Press, Baltimore (1999)
4. Burgess, N.: Spatial memory: How egocentric and allocentric combine. *Trends in Cognitive Sciences* 10, 551–557 (2006)
5. Wang, R.F., Spelke, E.: Human spatial representation: Insights from animals. *Trends in Cognitive Sciences* 6, 376 (2002)
6. Loomis, J.M., Klatzky, R.L., Golledge, R.G., Cicinelli, J.G., Pellegrino, J.W., Fry, P.A.: Nonvisual navigation by blind and sighted: Assessment of path integration ability. *Journal of Experimental Psychology - General* 122, 73–91 (1993)
7. Klatzky, R.L., Loomis, J.M., Golledge, R.G., Cicinelli, J.G., Doherty, S., Pellegrino, J.W.: Acquisition of route and survey knowledge in the absence of vision. *Journal of Motor Behavior* 22, 19–43 (1990)
8. McNamara, T.P., Rump, B., Werner, S.: Egocentric and geocentric frames of reference in memory of large-scale space. *Psychonomic Bulletin & Review* 10, 589–595 (2003)
9. Avraamides, M.N., Klatzky, R.L., Loomis, J.M., Golledge, R.G.: Use of cognitive versus perceptual heading during imagined locomotion depends on the response mode. *Psychological Science* 15, 403–408 (2004)
10. Montello, D.R., Waller, D., Hegarty, M., Richardson, A.E.: Spatial memory of real environments, virtual environments, and maps. In: Allen, G.L. (ed.) *Human Spatial Memory: Remembering where*, pp. 251–285. Lawrence Erlbaum Associates, Mahwah (2004)
11. Shelton, A.L., Gabrieli, J.D.: Neural correlates of encoding space from route and survey perspectives. *Journal of Neuroscience* 22, 2711–2717 (2002)
12. Gramann, K., Müller, H.J., Eick, E.M., Schönebeck, B.: Evidence of separable spatial representations in a virtual navigation task. *Journal of Experimental Psychology - Human Perception and Performance* 31, 1199–1223 (2005)
13. Gramann, K., Müller, H.J., Schönebeck, B., Debus, G.: The neural basis of ego- and allocentric reference frames in spatial navigation: Evidence from spatio-temporal coupled current density reconstruction. *Brain Research* 1118, 116–129 (2006)
14. Bohbot, V.D., Lerch, J., Thorndycraft, B., Iaria, G., Zijdenbos, A.P.: Gray matter differences correlate with spontaneous strategies in a human virtual navigation task. *Journal of Neuroscience* 27, 10078–10083 (2007)
15. Gramann, K., El Sharkawy, J., Deubel, H.: Eye-movements during navigation in a virtual tunnel. *International Journal of Neuroscience* 119, 1755–1778 (2009)
16. Galati, G., Lobel, E., Vallar, G., Berthoz, A., Pizzamiglio, L., Le Bihan, D.: The neural basis of egocentric and allocentric coding of space in humans: A functional magnetic resonance study. *Experimental Brain Research* 133, 156–164 (2000)
17. Merriam, E.P., Genovese, C.R., Colby, C.L.: Spatial updating in human parietal cortex. *Neuron* 39, 361–373 (2003)
18. Cavanna, A.E., Trimble, M.R.: The precuneus: A review of its functional anatomy and behavioural correlates. *Brain* 129, 564–583 (2006)
19. Andersen, R.A., Snyder, L.H., Bradley, D.C., Xing, J.: Multimodal representation of space in the posterior parietal cortex and its use in planning movements. *Annual Reviews in Neuroscience* 20, 303–330 (1997)
20. Aguirre, G.K., D'Esposito, M.: Topographical disorientation: A synthesis and taxonomy. *Brain* 122, 1613–1628 (1999)
21. Seubert, J., Humphreys, G.W., Müller, H.J., Gramann, K.: Straight after the turn: The role of the parietal lobes in egocentric space processing. *Neurocase* 14, 204–219 (2008)

22. Vann, S.D., Aggleton, J.P.: Testing the importance of the retrosplenial guidance system: Effects of different sized retrosplenial cortex lesions on heading direction and spatial working memory. *Behavioural Brain Research* 155, 97–108 (2004)
23. Burgess, N., Maguire, E.A., Spiers, H.J., O’Keefe, J.: A temporoparietal and prefrontal network for retrieving the spatial context of lifelike events. *Neuroimage* 14, 439–453 (2001)
24. Ino, T., Inoue, Y., Kage, M., Hirose, S., Kimura, T., Fukuyama, H.: Mental navigation in humans is processed in the anterior bank of the parieto-occipital sulcus. *Neuroscience Letters* 322, 182–186 (2002)
25. Redish, A.D.: Beyond the cognitive map: From place cells to episodic memory. The MIT Press, Cambridge (1999)
26. McNaughton, B.L., Battaglia, F.P., Jensen, O., Moser, E.I., Moser, M.B.: Path integration and the neural basis of the ‘cognitive map’. *Nature Reviews Neuroscience* 7, 663–678 (2006)
27. Hafting, T., Fyhn, M., Molden, S., Moser, M.B., Moser, E.I.: Microstructure of a spatial map in the entorhinal cortex. *Nature* 436, 801–806 (2005)
28. Maguire, E.A., Burgess, N., Donnett, J.G., Frackowiak, R.S., Frith, C.D., O’Keefe, J.: Knowing where and getting there: A human navigation network. *Science* 280, 921–924 (1998)
29. Jensen, O., Tesche, C.D.: Frontal theta activity in humans increases with memory load in a working memory task. *European Journal of Neuroscience* 15, 1395–1399 (2002)
30. Bischof, W.F., Boulanger, P.: Spatial navigation in virtual reality environments: An EEG analysis. *CyberPsychology and Behavior* 6, 487–495 (2003)
31. Klimesch, W.: EEG alpha and theta oscillations reflect cognitive and memory performance: A review and analysis. *Brain Research Reviews* 29, 169–195 (1999)
32. Lehmann, D., König, T.: Spatio-temporal dynamics of alpha brain electric fields, and cognitive modes. *International Journal of Psychophysiology* 26, 99–112 (1997)
33. Pfurtscheller, G., Lopez da Silva, F.H.: Event-related EEG/MEG synchronization and desynchronization: Basic principles. *Clinical Neurophysiology* 110, 1842–1857 (1999)
34. Onton, J., Makeig, S.: Information-based modeling of event-related brain dynamics. In: Neuper, C., Klimesch, E. (eds.) *Progress in Brain Research*, vol. 159, pp. 99–120 (2006)
35. Onton, J., Westerfield, M., Townsend, J., Makeig, S.: Imaging human EEG dynamics using independent component analysis. *Neuroscience and Biobehavioral Reviews* 30, 808–822 (2006)
36. Makeig, S., Bell, A.J., Jung, T.P., Sejnowski, T.J.: Independent component analysis of electroencephalographic data. *Advances in Neural Information Processing Systems* 8, 145–151 (1996)
37. Oostenveld, R., Praamstra, P.: The five percent electrode system for high-resolution EEG and ERP measurements. *Clinical Neurophysiology* 112, 713–719 (2001)
38. Delorme, A., Makeig, S.: EEGLAB: An open source toolbox for analysis of single-trial EEG dynamics including independent component analysis. *Journal of Neuroscience Methods* 134, 9–21 (2004)
39. Lee, T.W., Girolami, M., Sejnowski, T.J.: Independent component analysis using an extended infomax algorithm for mixed subgaussian and supergaussian sources. *Neural Computation* 11, 417–441 (1999)
40. Oostenveld, R., Oostendorp, T.F.: Validating the boundary element method for forward and inverse EEG computations in the presence of a hole in the skull. *Human Brain Mapping* 17, 179–192 (2002)

41. Makeig, S.: Auditory event-related dynamics of the EEG spectrum and effects of exposure to tones. *Electroencephalography and Clinical Neurophysiology* 86, 283–293 (1993)
42. Makeig, S., Debener, S., Onton, J., Delorme, A.: Mining event-related brain dynamics. *Trends in Cognitive Sciences* 8, 204–210 (2004)
43. Gramann, K., Onton, J., Riccobon, D., Müller, H.J., Bardins, S., Makeig, S.: Human brain dynamics accompanying the use of egocentric and allocentric reference frames during spatial navigation. *Journal of Cognitive Neuroscience* (in press)
44. Gevins, A., Smith, M.E., McEvoy, L., Yu, D.: High-resolution EEG mapping of cortical activation related to working memory: Effects of task difficulty, type of processing, and practice. *Cerebral Cortex* 7, 374–385 (1997)
45. Lancaster, J.L., Woldorff, M.G., Parsons, L.M., Liotti, M., Freitas, C.S., Rainey, L., Kochunov, P.V., Nickerson, D., Mikiten, S.A., Fox, P.T.: Automated Talairach atlas labels for functional brain mapping. *Human Brain Mapping* 10, 120–131 (2000)
46. Brodmann, K.: Vergleichende Lokalisationslehre der Grosshirnrinde: In ihren Prinzipien dargestellt auf Grund des Zellenbaues. Johann Ambrosius Barth Verlag, Leipzig (1925)
47. Harris, I.M., Egan, G.F., Sonkkila, C., Tochon-Danguy, H.J., Paxinos, G., Watson, J.D.G.: Selective right parietal lobe activation during mental rotation - A parametric PET study. *Brain* 123, 65–73 (2000)
48. Morrone, M.C., Tosetti, M., Montanaro, D., Fiorentini, A., Cioni, G., Burr, D.C.: A cortical area that responds specifically to optic flow, revealed by fMRI. *Nature Neuroscience* 3, 1322–1328 (2000)
49. Calton, J.L., Taube, J.S.: Where am I and how will I get there from here? A role for posterior parietal cortex in the integration of spatial information and route planning. *Neurobiology of Learning and Memory* 91, 186–196 (2009)
50. Field, D.T., Wilkie, R.M., Wann, J.P.: Neural systems in the visual control of steering. *Journal of Neuroscience* 27, 8002–8010 (2007)
51. Andersen, R.A.: Encoding of intention and spatial location in the posterior parietal cortex. *Cerebral Cortex* 5, 457–469 (1995)
52. Klimesch, W., Doppelmayr, M., Schwaiger, J., Auinger, P., Winkler, T.: 'Paradoxical' alpha synchronization in a memory task. *Cognitive Brain Research* 7, 493–501 (1999)
53. Kahana, M.J., Sekuler, R., Caplan, J.B., Kirschen, M., Madsen, J.R.: Human theta oscillations exhibit task dependence during virtual maze navigation. *Nature* 399, 781–784 (1999)
54. Caplan, J.B., Madsen, J.R., Schulze-Bonhage, A., Aschenbrenner-Scheibe, R., Newman, E.L., Kahana, M.J.: Human theta oscillations related to sensorimotor integration and spatial learning. *Journal of Neuroscience* 23, 4726–4736 (2003)
55. Makeig, S., Gramann, K., Jung, T.P., Sejnowski, T., Poizner, H.: Linking brain, mind and behavior. *International Journal of Psychophysiology* 73, 95–100 (2009)